

Aerodynamic Analysis and Comparison of Swallow and Pipette Birds

M.Z. Abdullah , H. Yusoff, M.R. Mat Nawi, M.Z. Mansor, Z. Mohd Ripin and R.

Ahmad

School of Mechanical Engineering, Universiti Sains Malaysia, Engineering Campus,
14300 Nibong Tebal, Penang, Malaysia.

Abstract

U E MAGAL

29948

Aerodynamic theory provides an approach to study flight design of birds and also to examine the evolutionary design of their morphology. Recent research has obtained the aerodynamic performance of swallow and pipette bird and also analyzed the air flow around the bodies and wings. Aerodynamic performance of swallow bird (*hirundo rustica*) and pipette bird (*scaly-breasted munia*) has been obtained experimentally. Swallow bird has been studied at two Reynolds numbers; i.e. 4.44×10^4 (12 m/s) and 4.81×10^4 (13 m/s) whereas pipette bird (*scaly-breasted munia*) at Reynolds numbers 2.88×10^4 and 3.11×10^4 corresponding to 12 m/s and 13 m/s respectively. As results, it has clearly shown that swallow bird has the ability to get better lift compared to the pipette bird when they fly at same speed and angle of attack. In terms of drag, swallow has less than pipette but the swallow's drag turns to higher value when it reached near the stall angle. A 3-dimensional simulation using a Computational Fluid Dynamic (CFD) code, FLUENT 6.0 is run under same conditions as in the wind tunnel test section. The simulation is done to predict the aerodynamics performance and also to illustrate pressure contour and velocity vector around the bird's body. Simulation results and experimental results have shown a fairly good agreement. Meanwhile, the pressure contours and velocity vectors have shown that the Bernoulli's principle is obeyed.

Keywords: Bird Flight; Reynolds Number; Lift Coefficient; Drag Coefficient; Computational Fluids Dynamics.

1. Introduction

Study of bird's flight is now come out very interesting when the study involved the several types of birds in the world. Each type of bird has their own flight characteristics applicable for their nature of life. Therefore, the comparison analysis can be made to collect data to optimize the development of any flying machine. In the past, different points of view have been adopted to conduct flight of bird's studies, depending on the background education and the personal interest of the scientists involved. Meseguer et al. (2003) have studied the alula effect for high lift device. The influence of the alula in the wing aerodynamics is similar to that of leading edge slats in aircraft wing, which are only operating during take-off and landing operations. Ramakrishnanda and Wong (1999) have investigated on animating bird flight using aerodynamics. They employed aerodynamic principles for the physical animation of bird flight. Hedenstrom (2002) has studied on aerodynamics, evolution and ecology of avian of flight using sophisticated techniques, has generated new and exciting insights about the evolution of flight, the function of tails and the ecological adaptations to a flying lifestyle. One of the aerodynamic advantages of bird flight is 'V' formation flying (P. Seiler et al., 2003). The theory would be confirm if it is observed that the variation in wing tip spacing is larger for birds farther form the leader than for the birds closer to the leader. Lissaman and Shollenberger (1970) have revealed that birds gain some aerodynamic advantage when in a linear formations such as the 'V', 'J' or echelon. Most of the past researchers used the

wind tunnel test to investigate the aerodynamics lift and drag around wing airfoil. With the improvement of computer technology and performance, the prediction of two-dimensional and three-dimensional flow structures can be made cheaply and consumed less time for analysis. This paper presents the comparison results between aerodynamic performances of swallow and pipette bird by using experimental investigation. Beside that, computer simulation has been done in order to consolidate the experimental results. The results of three-velocity components and pressure contours for several Reynolds number also are presented in this paper.

2. Birds (swallow and pipette) and wings characteristics

Swallow bird or specific named as barn swallow (*hirundo rustica*) is a small perching bird found almost everywhere in the world. They are small type of bird and having long narrow wings, forked tail and weak feet. Therefore, they can make abrupt changes a top speed in different directions during flying. Pipette bird or scientifically named as *scaly-breasted munia* are now quite common in Malaysia and Singapore. They are found even in urban areas as well as cultivated lands, grasslands, scrub and secondary growth. Rapid fluctuating flight and gliding into cover are the flight characteristics of pipette bird.

To analyze the flight of birds from an engineering point of view, in an extreme simplification of the problem, it can be said that birds can fly either by gliding or by flapping. The aerodynamics of wing sections is a complex problem in fluid mechanics that is satisfactorily solved at present. However, the analysis of the fluid movement

around an airfoil of bird's wing requires both experimental testing and computer simulation for faster and cheaper technique for analysis.

Tricker and Tricker (1967) have revealed that the bird's wing is similar to the human arm in many aspects. Both comprise shoulder, elbow and wrist joints followed by metacarpals (fingers). The portion of the wing between the shoulder joint and the elbow joint is not aerodynamically significant for most birds and can be neglected in calculations. The cross-section of a bird's wing is quite similar to the aerofoil section of an aircraft (Houghton and Carruthers, 1982). The reader is referred to Tricker and Tricker (1967) for the anatomical details of a bird's flight muscles and to Anderson (1991) for definitions of the aerofoil parameters.

In years 1997 and 1998, several parameters of the wing geometry of almost four hundred and fifty birds, belonging to forty different species living in Spain, have been measured (the biometry method has been published elsewhere, Alvarez et al., 1997). The following parameters are used to obtain the characteristic of bird's wing as shown in Figure 1.

M = mass of the bird

S_b = total lifting surface

S_w = wing area

From these contours, the wing area, S_w and the total lifting surface of each bird S_b , have been obtained (the total lifting surface S_b has been defined according to Pennycuick (1989), as $S_b = 2S_w + L_t c_w$, where L_t is the width of the thorax, $L_t = L_b - 2L_w$, wing load $W_l = Mg/S_b$ and to the wing geometry, the bird aspect ratio, $AR = L_b^2/S_b$). Three birds for each swallow and pipette birds have been taken as the samples in the present study in order to obtain the average values of wing load, wing area and aspect ratio. These average values are indicated in Table 1 and Table 2.

Table 1: Characteristics of wing shape of swallow bird

Number of samples	Wing Load $W_l = Mg/S_b$ (mN/cm ²)	Wing Area, S_w (cm ²)	Aspect Ratio $AR = L_b^2/S_b$
1	0.140	66.5	9.778
2	0.146	70	9.657
3	0.186	69	9.647
Average	0.157	68.5	9.694

Table 2: Characteristics of wing shape of pipette bird

Number of samples	Wing Load $W_l = Mg/S_b$ (mN/cm ²)	Wing Area, S_w (cm ²)	Aspect Ratio $AR = L_b^2/S_b$
1	0.27	37.63	4.70
2	0.34	35.50	4.91
3	0.30	36.40	4.64
Average	0.30	36.51	4.75

According to the wing shapes classification proposed by Saville (1956), there are many types of wings as indicated in Table 3.

Table 3: Wing shape classification

Wing shapes classification	Functions
Elliptical wing (recommended for pipette's wing)	<ul style="list-style-type: none"> • Wing shape is very efficient at low and moderate speeds. • Generate smooth tip vortex and uniform pressure distribution over the wing surface. • Provide good maneuverability and it is characteristic of small birds with active flight.
High speed wing	<ul style="list-style-type: none"> • It is characterized by low camber airfoils, moderate high aspect ratio, pronounced sweepback of the leading edge. • Wing tip is not generally slotted. • Moving in open spaces has this type of wing with high flight speeds.
High aspect ratio wing (recommended for swallow's bird)	<ul style="list-style-type: none"> • Typical wing of the birds that use to fly over water surfaces. • High aerodynamic efficiency and could be labeled also high speed soaring wings.
High lift	<ul style="list-style-type: none"> • Characterized by slotted wing tip, moderate aspect ratio and pronounced camber airfoils. • Very efficient at low speeds and they seems to be

wing	<p>especially adapted for soaring flight over the land.</p> <ul style="list-style-type: none"> This wing could be also described as low speed soaring wings.
------	---

3. Experimental Set-up

Recent research has been done experimentally in a low speed and open circuit wind tunnel (Figure 2). The wind tunnel has a 300mm x 300mm x 600mm Plexiglas test section with three components electronic balancing unit for the measurement of lift, drag and pitching moment. A preserved swallow and pipette bird with the feathers on has been located in the middle of the test section. The velocity in the wind tunnel has been measured by using Pitot tube. The maximum velocity in the test section is 38 m/s. The test was conducted at Reynolds numbers from 28800 to 48100. The birds have been rotated at different angles of attack from -36° to 36° .

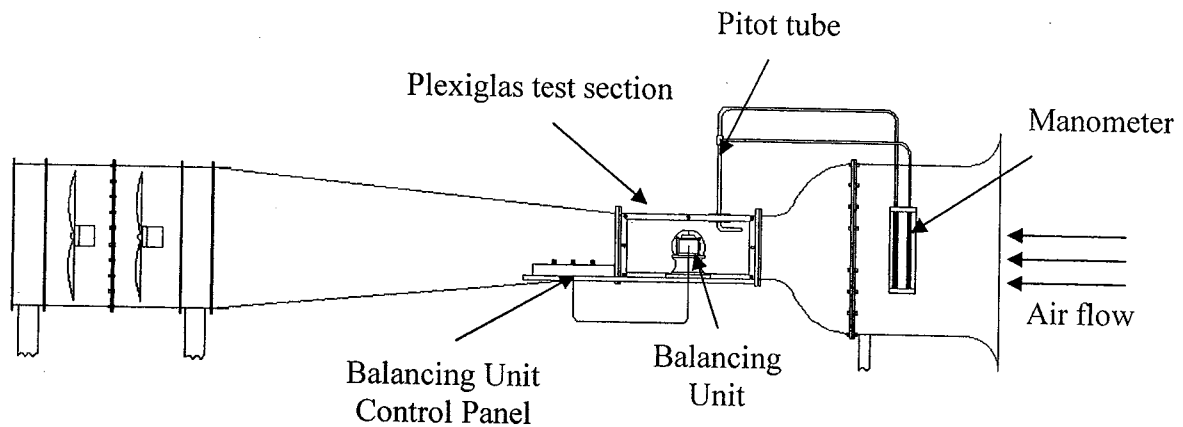


Figure 2: Low speed open circuit wind tunnel

3.1 Formulation and simulation setup

The steady flow of a viscous incompressible fluid flow around a bird is considered. The basic equations used in the simulation are the equation of continuity and the Navier-Stokes equations:

$$\vec{\nabla} \cdot \vec{V} = 0 \quad (5)$$

$$(\vec{V} \cdot \vec{\nabla})\vec{V} = -\frac{1}{\rho}\vec{\nabla}P + \nu\nabla^2\vec{V} \quad (6)$$

$$\text{where } \vec{\nabla} = \frac{\partial}{\partial x} + \frac{\partial}{\partial y} + \frac{\partial}{\partial z}$$

CFD software FLUENT 6.0 and the pre-processor software GAMBIT 1.2 are used in the investigation to predict the lift and drag coefficients. The simulation followed the same condition as in wind tunnel. Unstructured meshes are used to model a bird without considering its' feathers to avoid complexity in the modeling. In meshing process, the need to reduce the time required to design and develop a configuration often required the users to obtain solution on computational meshes that are relatively small although computer's speeds and memory sizes have increased, allowing the solution of larger flow problem as proposed by Van Dam (1999). For the turbulence analysis, the k - ϵ model is used in the investigation. The mesh generated around bird is shown in Figure 3.

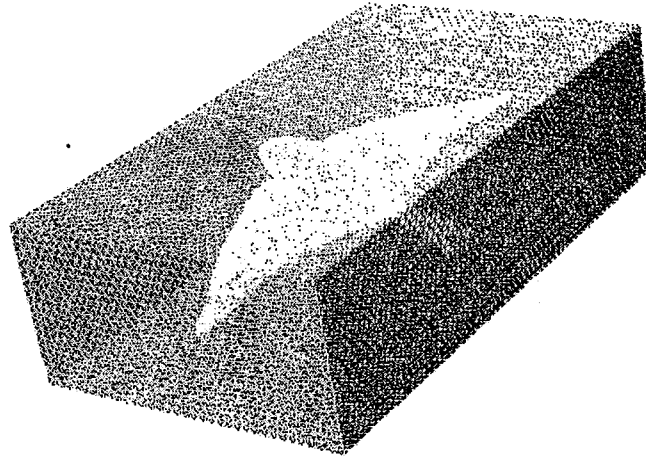


Figure 3: Mesh around swallow bird

The k- ϵ turbulence model is used in order model the turbulence. The equations describing the relationship between turbulence intensity and turbulence kinetic energy, k and turbulence dissipation rate, ϵ as follow:

$$k = \frac{3}{2}(U \times TI)^2 \quad (7)$$

$$\epsilon = C_\mu^{\frac{3}{4}} \frac{k^{\frac{3}{2}}}{l} \quad (8)$$

where $C_\mu = 0.09$

l = turbulence length scale $\approx 0.07C_w$

C_w = maximum wing chord

U = free stream velocity

TI = turbulence intensity

The maximum wing chord is taken as the characteristic length, C_w .

4. Results and Discussion

4.1 Results comparison between swallow and pipette bird

The experiments in the wind tunnel for both swallow and pipette bird have been carried out at Reynolds numbers from 2.88×10^4 till 4.81×10^4 and at various angles of attack, α from -36° to 36° . The comparisons of results presented are lift, drag, drag polar and lift to drag ratio curves.

Experiments of lift for both birds are done in the wind tunnel at 13 m/s. Due to the different of maximum wing chord, C_w ($C_{w\text{swallow}} = 0.048$ m and $C_{w\text{pipette}} = 0.035$ m), the Reynolds number for swallow is 4.81×10^4 whereas 3.11×10^4 for pipette. The comparison of lift coefficient between these two birds is presented in Figure 4. Generally, both curves show the same profile. The increment is continuous until the angle of attack reaches the stall angle. After that, the lift coefficient is reduced. Lift coefficients value of swallow has shown higher than pipette. The maximum lift coefficient, $C_{L\text{max}}$ of swallow is 0.92 at stall angle, $\alpha_{\text{stall}} = 32^\circ$ while pipette is 0.89 occurred at $\alpha_{\text{stall}} = 27^\circ$. Stall angle of swallow is higher than pipette because of swallow has wing shape similar to the sweep back delta wing of aircraft meanwhile the pipette's wing is identified as elliptical wing. Theoretically, common aircraft attached with sweep back delta wing takes higher degree during take off compared to the other aircrafts at same speed. At $\alpha = 0^\circ$, the C_L of swallow is 0.14 whereas $C_L = 0.06$ for pipette. It shows that swallow is flying higher than pipette at same speed. In Figure 4, it also has shown that the decreasing of lift coefficient after stall angle of pipette bird (about 5.5%) is lower than swallow bird (about 8.6%).

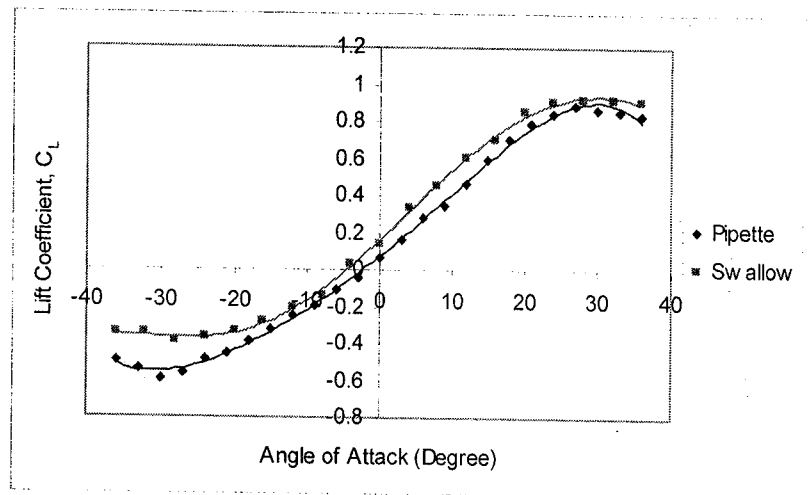


Figure 4: Comparison of lift coefficient curves

Figure 5 presents the comparison of drag coefficient against angle of attack between swallow and pipette at 13 m/s (swallow, $Re = 4.81 \times 10^4$ and pipette, $Re = 3.11 \times 10^4$) speed. The results indicate that the drag coefficient of pipette and swallow is increased with the angle of attack increases. The increment of C_D for pipette is more gradual than swallow despite the C_D of swallow is lower than pipette at $\alpha = 0^\circ$. As a result, the C_D of swallow is higher than pipette at the stall angle. After the stall angle, drag coefficient of both birds is slightly increased (swallow (20.4%) and pipette (10%)).

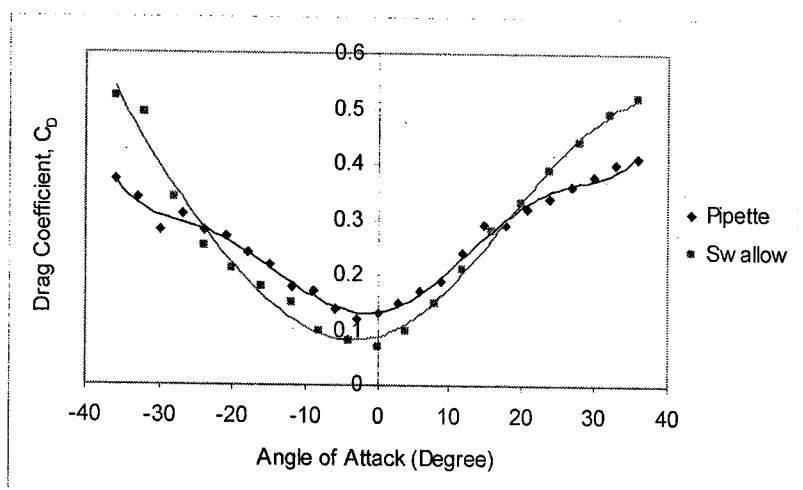


Figure 5: Comparison of drag coefficient curves

The drag polar of both swallow and pipette birds at 13 m/s speed are presented in Figure 6. Drag polar characteristic is important to describe the aerodynamic performance. Figure 6 indicates that the $C_{Lmax} = 0.92$ at $C_D = 0.49$ for swallow bird and $C_{Lmax} = 0.9$ at $C_D = 0.38$ for pipette bird.

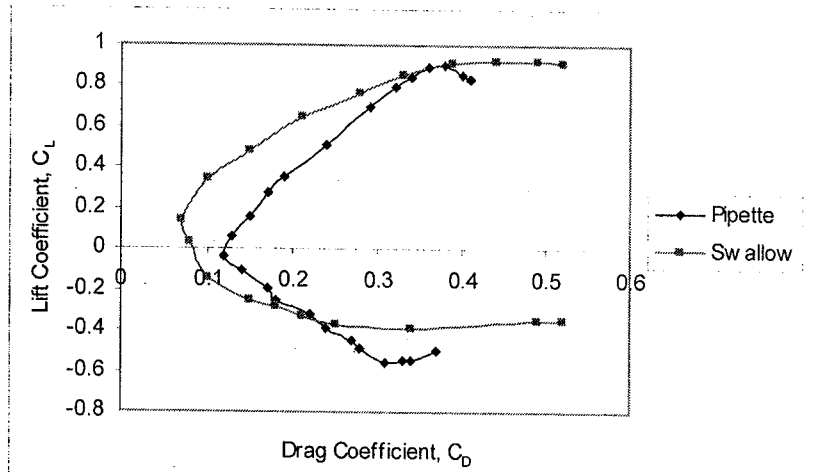


Figure 6: Comparison of drag polar curves

The relation between lift to drag ratio and angle of attack for the two birds at 13 m/s speed is shown in Figure 7. The aerodynamic efficiency of swallow ($Re = 4.81 \times 10^4$) and pipette ($Re = 3.11 \times 10^4$) bird can be compared by referring to Figure 7. In the application of aircraft design, lift to drag ratio is an important parameter to obtain the most suitable thrust required at certain speed. Therefore, right choosing of aerodynamic design is definitely needed to enhance the aircraft performance. Lift to drag ratio indicates that the minimum thrust required at certain velocity is at maximum L/D . The L/D_{max} of swallow bird is at 3.0 at $\alpha = 8^\circ$ whereas pipette has shown its $L/D_{max} = 0.89$ at $\alpha = 27^\circ$. It indicates that minimum thrust required for swallow and pipette bird at $\alpha = 8^\circ$ (before stall angle) and $\alpha = 27^\circ$ (stall angle) respectively.

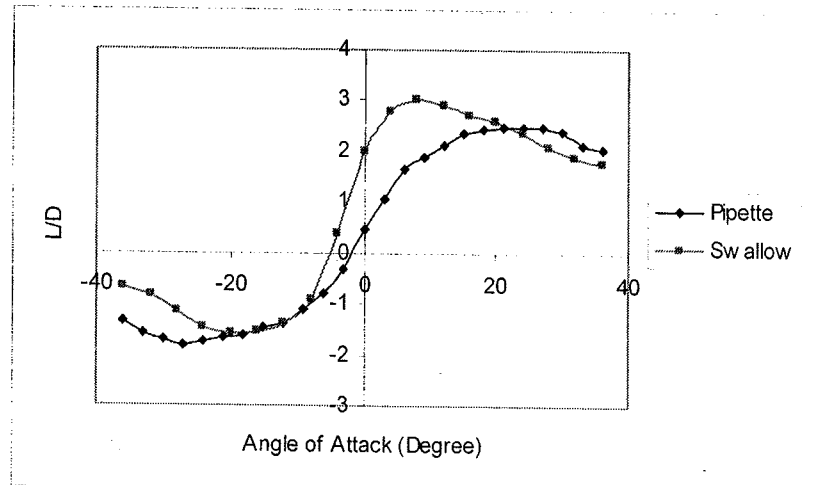


Figure 7: Comparison of lift to drag curves

4.2 Lift and drag coefficients of swallow bird analysis

The lift coefficient of swallow bird obtained from experiment under two Reynolds numbers are shown in Figure 8. Both curves show that the lift coefficient is increased when the angle of attack increases. This increment is continuous until the angle of attack reaches the stall angle. After that, the lift coefficient is reduced. The results obtained show similar trends for common airfoil or aircraft wings. At $\alpha = 0$, the C_L is 0.14 for $Re = 4.4 \times 10^4$ (12 m/s) and 0.13 for $Re = 4.81 \times 10^4$ (13 m/s). The maximum lift coefficient, $C_{L_{max}}$ is occurred at $\alpha = 32^\circ$. This stall angle is higher (delayed) compared to the common aircraft wing around 12° - 20° . One of the reasons may be due the effect of feathers around the swallow bird. The $C_{L_{max}}$ for $Re = 4.44 \times 10^4$ is 0.97 and for the $Re = 4.81 \times 10^4$, the $C_{L_{max}}$ is 0.93. Up to $\alpha = 36^\circ$, the lift coefficient suddenly decreased. The lift coefficient decreases approximately 5.15% ($Re = 4.44 \times 10^4$) and 8.6% ($Re = 4.81 \times 10^4$) lower than the maximum lift coefficient.

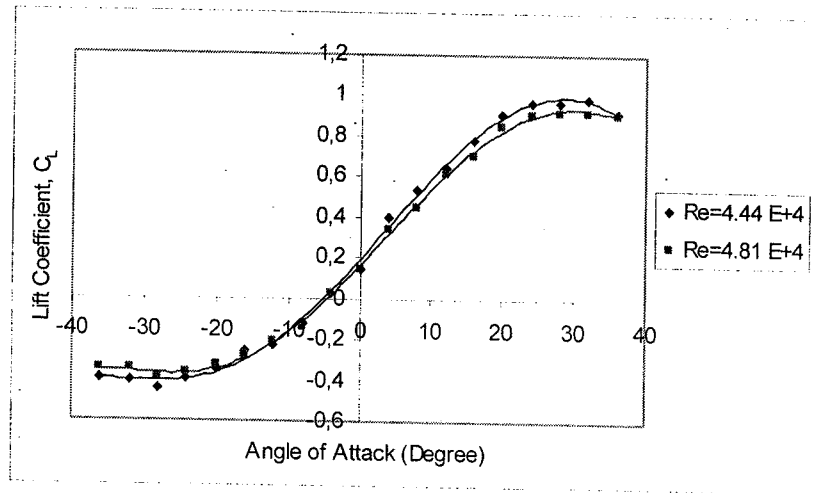


Figure 8: Swallow lift curves

Figure 9 shows the drag coefficient of swallow bird against the angle of attack. The results indicate that the drag coefficient is increased gradually with the angle of attack increases where the trends of the result like as a 'V' shape. The increment is approximately 21.8% and 20.4% for $Re = 4.44 \times 10^4$ and $Re = 4.81 \times 10^4$ respectively. At $\alpha = 0^\circ$, the drag coefficients of swallow bird are 0.03 ($Re = 4.44 \times 10^4$) and 0.07 ($Re = 4.81 \times 10^4$). Whereas, at stall angle ($\alpha = 32^\circ$), the C_D are 0.38 ($Re = 4.44 \times 10^4$) and 0.49 ($Re = 4.81 \times 10^4$).

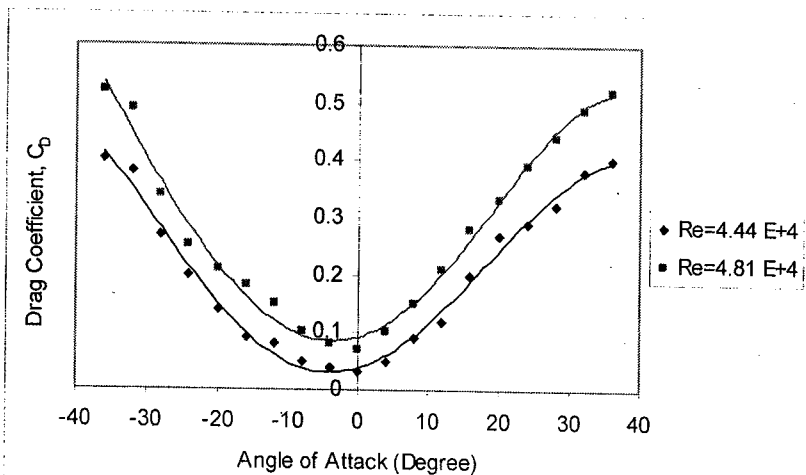


Figure 9: Swallow drag curves

4.3 Lift and drag coefficients of pipette bird analysis

Next analysis is to analyze the lift coefficient curve of pipette bird at two Reynolds numbers as indicated in Figure 10. The profile shows that the lift coefficient is increased continuously when the angle of attack increases until the stall angle. After that, the lift coefficient is reduced. At $\alpha = 0$, the C_L is 0.08 for $Re = 2.88 \times 10^4$ (12 m/s) and 0.06 for $Re = 3.11 \times 10^4$ (13 m/s). The maximum lift coefficient, C_{Lmax} is occurred at $\alpha = 30^\circ$. Same as swallow wing, the stall angle of pipette is higher (delayed) compared to the common aircraft wing around 12° - 20° . The effect of feathers around the swallow bird may be affected the results. The C_{Lmax} for $Re = 2.88 \times 10^4$ is 0.87 and for the $Re = 3.11 \times 10^4$, the C_{Lmax} is 0.9. Up to $\alpha = 36^\circ$, the lift coefficient suddenly decreased. The lift coefficient decreases approximately 4.59% ($Re = 2.88 \times 10^4$) and 5.55% ($Re = 3.11 \times 10^4$) lower than the maximum lift coefficient.

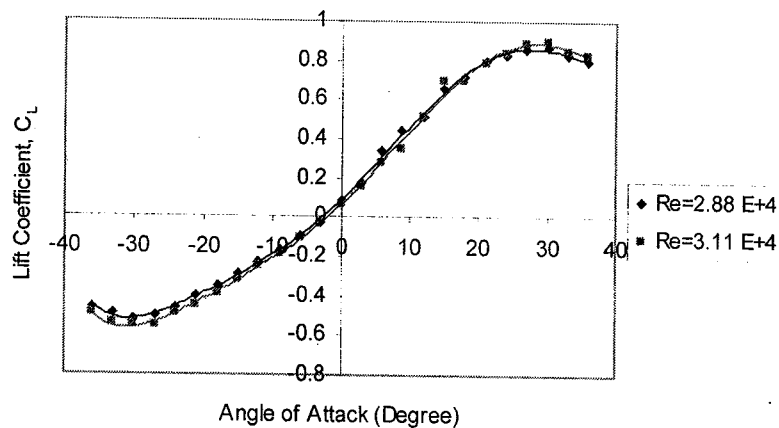


Figure 10: Pipette lift curves

Analysis of the pipette's drag coefficient against the angle of attack is shown in Figure 11. The results indicate that the drag coefficient of $Re = 2.88 \times 10^4$ (12 m/s) is increased more gradual than $Re = 3.11 \times 10^4$ (13 m/s) with the angle of attack increases. As results, at $\alpha = 0^\circ$, the drag coefficients are 0.09 ($Re = 2.88 \times 10^4$) and 0.13 ($Re = 3.11 \times 10^4$) whereas at $\alpha = 30^\circ$ (stall angle), the drag coefficients are 0.42 ($Re = 2.88 \times 10^4$) and 0.38 ($Re = 3.11 \times 10^4$).

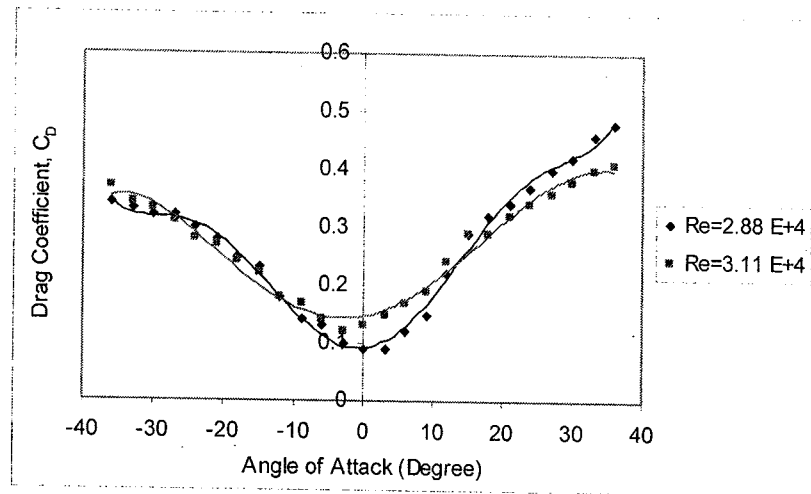


Figure 11: Pipette drag curves

4.4 Comparison between experimental and simulation results

Next discussion is to consolidate recent study by comparing experimental results with the simulation results. In this paper, the comparison between these two results has been done for swallow bird at $Re = 4.44 \times 10^4$. This comparison is enough to estimate the relationship between experimental and computational simulation results of pipette bird. Figures 12 and 13 are presented the comparison experimental and simulation results of swallow's lift and drag coefficients at $Re = 4.44 \times 10^4$. In Figure 12, two curves experimental and simulation results of swallow's lift coefficient

show a similar trend. The trend shows the value of C_L is increased when the angle of attack increasing. But, the C_L is immediately decreased after the stall angle for the experimental result. Figure 12 also shows the lift slope for experimental results are 0.028 per degree and 0.031 per degree for simulation result. The value of simulation result predicted about 9.6% lower than the experimental result. The difference occurs due to the effect of swallow feather gave higher lift coefficient for experimental results, whereas in the simulation, the bird with no feathers is used. However, the simulation results are shown still fairly good agreement with the experimental results.

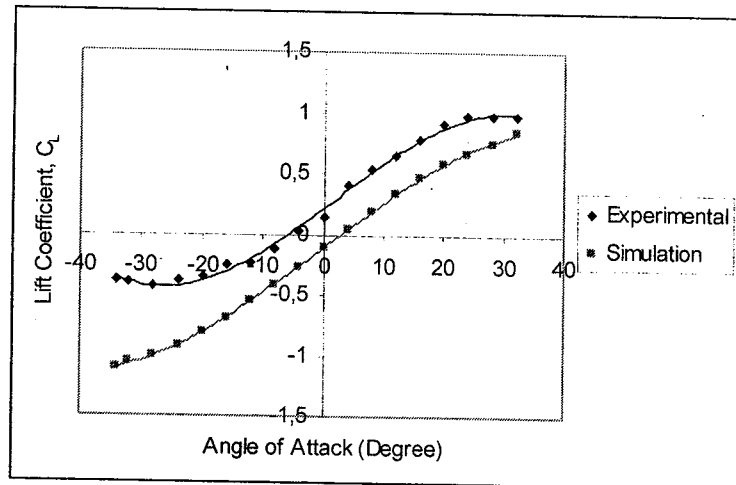


Figure 12: Swallow lift curves obtained from experiment and simulation

The comparison of swallow drag curves between simulation and experimental are shown in Figure 13. The pattern shows of the two graphs are similar trends. The experimental drag curve is lower than the simulation drag curve. The drag slope for simulation result is 0.016 per degree while 0.013 per degree for experimental result. In average, the experimental result is about 18% lower than the simulation results. The simulation and experimental results are shown a good agreement. Again the

differences due to the effect of swallow feathers in the experimental results have delayed the separation and reduce drag friction coefficient.

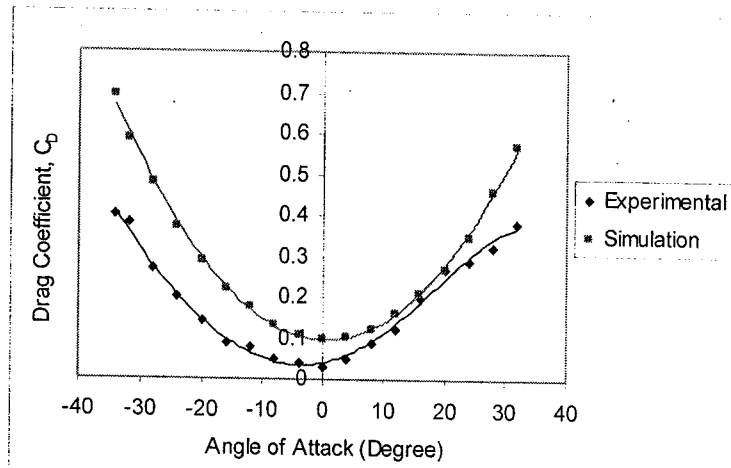


Figure 13: Swallow drag curves obtained from experiment and simulation

4.3 Pressure contour and velocity vector

In the simulation, two parameters have been considered; i.e. pressure contour and velocity vector. In pressure contour, the result shows the general pressure distribution around the body and wings of swallow bird when it is subjected to a certain angle of attack and different Reynolds numbers. Generally, pressure contour indicates that the highest pressure is occurs at the beak of the bird locating in front of the body. The pressure also high at the wing leading edge, but the pressure is low at the wing tip. At the upper surface of the body and wing, the pressure is lower compared to the front and lower of the body surfaces.

Investigation on pressure contour and velocity vector around bird's body has been done for swallow bird at $\alpha = 8^\circ$ (lowest L/D ratio) as illustrated in Figures 14

and 15. In Figure 14, the stagnation point move backward to the lower surface and the highest pressure region is growing. The highest pressure (about 2.51×10^2 Pa) is occurred at beak and at the wing leading edge whereas the lowest pressure region approximately -1.35×10^2 Pa is located at the wing upper surface near the body.

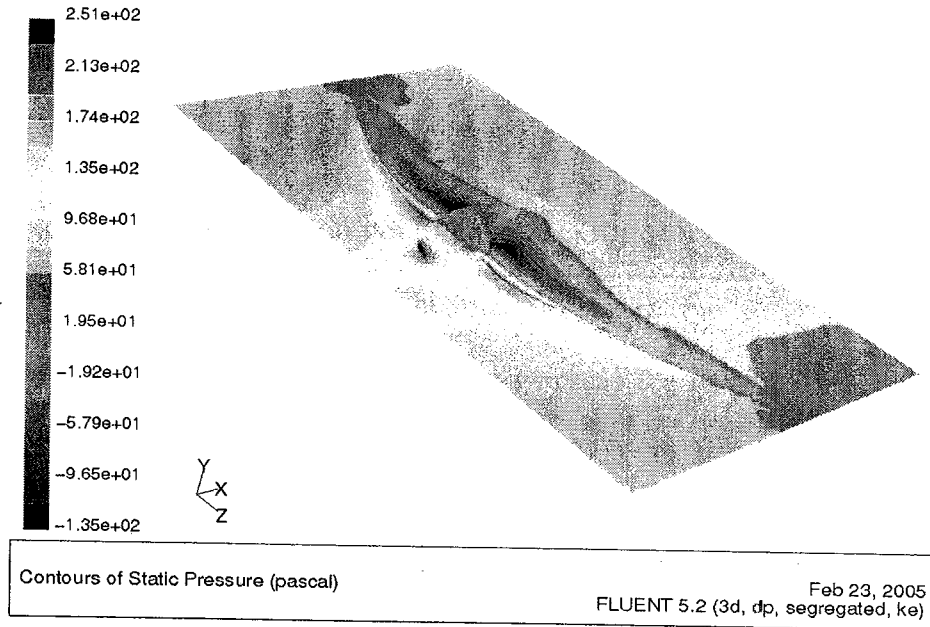


Figure 14: Swallow's pressure contour at $\alpha = 8^\circ$

Velocity vector of swallow bird at $\alpha = 8^\circ$ (lowest L/D ratio) is presented in Figure 15. It shows that the velocity is low (about 7.1 m/s) at the lower surface and the leading edge wing. The lowest velocity (about 2.0 m/s) occurs at between body and tail, meanwhile the highest velocity (about 20 m/s) occurs at the mid of upper surface wing. The highest velocity value is increased about 38% compare to the free stream velocity.

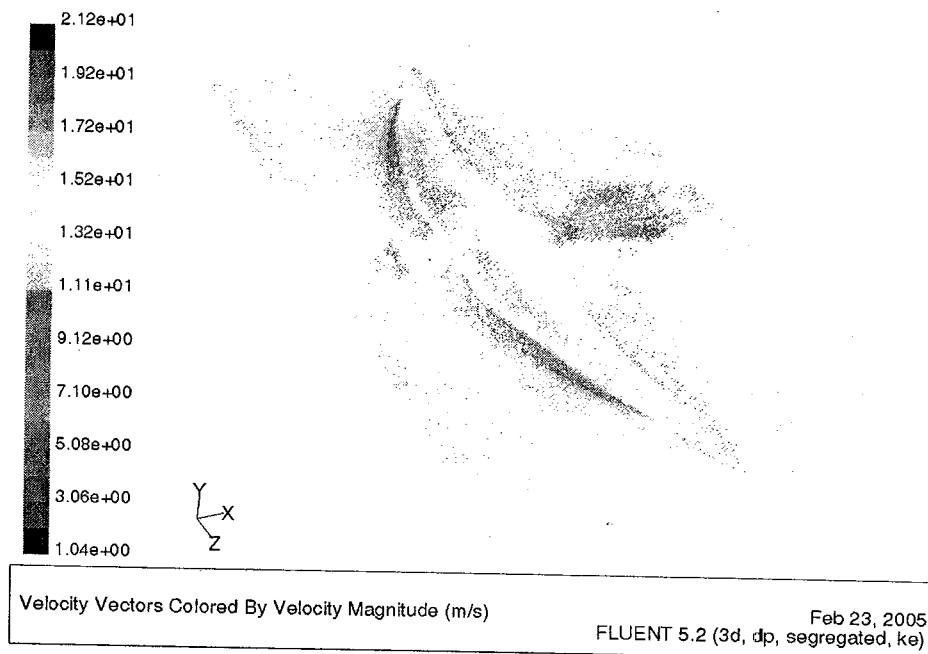


Figure 15: Swallow's velocity vector at $\alpha = 8^\circ$

5. Conclusion

The aerodynamic characteristics of swallow and pipette bird are being analyzed and compared each others in this paper. The study has involved wind tunnel experiment and computer simulation. As results, it has clearly shown that swallow bird has the ability to get better lift compared to the pipette bird when they fly at same speed and angle of attack. Whereas, swallow has lower than pipette in term of drag at level ($\alpha = 0^\circ$) flight. But, the increment of swallow's drag is higher than pipette's drag. Therefore, the drag coefficient of swallow is higher than pipette at stall angle.

Computer simulation has been done in order to consolidate the experimental results. The simulation results are limited due to the bird model has made with no feathers attached. Overall, the comparison between simulation and experimental results are shown a fairly good agreement. The contours illustrate that high velocity

and low pressure are occurred at the upper wing and wing tip meanwhile the parts like beak, trailing and leading edge, lower wing and also tails have low velocity and high pressure in nature. As conclusion, contours illustrations are obeyed the Bernoulli's principle.

Nomenclature

AR	aspect ratio
C_D	drag coefficient
C_L	lift coefficient
C_{Lmax}	maximum lift coefficient
C_w	maximum wing chord (cm)
d	the interval size
k	kinetic energy of turbulence
l	turbulence length scale
L_a	length of the alula (cm)
L_b	bird span (cm)
L_c	distance between the root of the alula and the wing tip (cm)
L_t	length of thorax (cm)
L_w	length of the extended wing (cm)
L/D	lift to drag ratio
M	mass of the bird (g)
n	the number of the intervals on the edge

Re	Reynolds number
S_b	total lifting surface (cm^2)
S_w	wing area (cm^2)
TI	turbulence intensity
U	free stream velocity
W_l	wing load (mN/cm^2)

Greek symbols

α	angle of attack (degree)
ε	dissipation of turbulence kinetic energy
ρ	density (kg/m^3)
μ	dynamic viscosity ($kg/m-s$)

Acknowledgements

The authors wish to thanks the Universiti Sains Malaysia and the Ministry of Higher Education of Malaysia for their financial supports under the Fundamental Research Grant.

References

Anderson, J.D. (1991). 'Fundamentals of Aerodynamics'. (McGraw-Hill: New York.)

Alvarez, J.C., Perez, A. and Meseguer, J. (1998). Biometria de la pardela cenicienta calonectris diomedea y paino comun Hydrobates Pelagius, in Anuari Ornitológic de les Balears 1997 Volum 12 (in Spanish), pp. 17-28.

Hedenström, A. (2002). Aerodynamics, evolution and ecology of avian flight. *TRENDS in Ecology & Evolution*, Vol. 17 No. 9, 415-422.

Houghton, E.L., Carruthers, N.B. (1982). 'Aerodynamics for Engineering Students. (Arnolds: London.)

J. Meseguer, J.C. Alvarez, E. Meseguer, A. Perez (2003). The alula: a leading edge, high lift device of birds. (IDR/UPM, E.T.S.I. Aeronauticos, Universidad Politécnica de Madrid.)

Lissaman, P., Shollenberger, C. (1970). Formation flight of birds. *Science* **168**, 1003-1005.

P. Seiler, A. Pant, J.K. Herdick (2003). A systems interpretation for observations of bird V-formations. *Journal of Theoretical Biology* **221**, 279-287.

Pennycuik, C. (1989). Bird flight performance. A Practical Calculation Manual. (Oxford: Oxford University Press.)

Ramakrishnananda, B., Wong, K.C. (1999). Animating bird flight using aerodynamics. *The Visual Computer* **15**:494-508.

Saville, D.O.B. (1956). Adaptive evolution in avian flight. *Evolution* **11**, 212-214.